UMT PRESS

Journal of Sustainability Science and Management
Journal Homepage: https://jssm.umt.edu.my
eISSN: 2672-7226
DOI: http://doi.org/10.46754/jssm.2026.07.005

CORROSION INHIBITION EFFICACY OF DRUGS IN 1 M HCL MEDIUM ON CARBON AND MILD STEELS: EXPERIMENTAL AND THEORETICAL COMPARATIVE STUDY

CHAIMAE MERIMI[1], ABDESSAMAD BENABBOU[1], HICHAM MAHMOUD[1], ZAKARIAE ABBAOUI[1], HASSANE LGAZ[2], ALI DAFALI[1], WAN MOHD NORSANI WAN NIK[3], MOHD SABRI MOHD GHAZALI[4]*, NURSABRINA AMIRAH MOHD NASIR[4], ELYOR BERDIMURODOV[5], RACHID TOUZANI[1] AND BELKHEIR HAMMOUTI[6,7]

[1]*University Mohammed Premier, Faculty of Science, Laboratory of Applied Chemistry and Environment (LCAE), University Mohammed Premier, Bd. Med VI B.P. 717, 60000 Oujda, Morocco*
[2]*Innovative Durable Building and Infrastructure Research Center, Center for Creative Convergence Education, Hanyang University ERICA, 55 Hanyangdaehak-ro, Sangrok-gu, Ansan-Si 15588, Gyeonggi-do, Republic of Korea*
[3]*Faculty of Ocean Engineering Technology, Universiti Malaysia Terengganu, Kuala Nerus 21030, Terengganu, Malaysia*
[4]*Faculty of Science and Marine Environment, Universiti Malaysia Terengganu, Kuala Nerus 21030, Terengganu, Malaysia*
[5]*Chemical and Materials Engineering, New Uzbekistan University, 54 Mustaqillik Ave., Tashkent, 100007, Uzbekistan*
[6]*Euro-Mediterranean University of Fez, 2WVH+7R2, Rte Principale Fès Meknès, Fès, Morocco*
[7]*Laboratory of Industrial Engineering, Energy and the Environment (LI3E) SUPMTI, Rabat 10000, Morocco*

**Corresponding author: mohdsabri@umt.edu.my*

ARTICLE INFO

Article History:
Received: 18 May 2025
Revised: 30 April 2026
Accepted: 7 May 2026
Published: 15 July 2026

Keywords:
XC48 Steel, mild steel, drugs, corrosion inhibition, DFT, electrochemical techniques

ABSTRACT

Metals and alloys, despite their advantageous properties, can suffer from reduced corrosion resistance when exposed to certain environments, leading to high costs of repair or replacement. In reinforced concrete, the corrosion of steel reinforcements, particularly due to chloride ions, affects material durability. To mitigate the issue, this study evaluated the corrosion inhibition efficiency (EI%) of acetaminophen (A1) and acetylsalicylic acid (A2) on XC48 and mild steel in 1 M hydrochloric acid (HCl). Electrochemical and gravimetric methods showed that both inhibitors were effective, with a 5.10-3 M concentration yielding notable EI%. Adsorption followed the Langmuir model. Moreover, computational simulations based on Density Functional Theory (DFT) were also used in order to acquire a more in-depth and detailed understanding of how the inhibitor compounds form interactions with the metallic surface layers, with the aim of enhancing corrosion inhibition performance. The results highlight the importance of material management strategies and ongoing research to maximise the durability of metal structures, reduce environmental impacts and improve the efficiency of corrosion inhibition methods.

Introduction

Corrosion represents a ubiquitous process exerting a substantial impact across multiple sectors, leading to material degradation, increased maintenance costs and, in some cases, catastrophic failures. Cases of loss of material strength due to corrosive processes translate into huge financial implications, particularly in sectors such as building, logistics and industrial production. Over the years, various techniques that seek to reduce the consequences of such damage have been proposed and the use of corrosion inhibitors has consistently emerged as one of the most effective, efficient and cost-effective strategies of providing protective measures to metals against progressive destruction (Al-Amiery *et al.*, 2023; Eliboev *et*

al., 2023; Merimi *et al.*, 2024). The mechanism by which these types of corrosion inhibitors work is by forming a thin and protective layer along the metallic surface, so that the corrosion reaction would not take place even in cases where such inhibitors are used in relatively small concentrations. In most cases, their mechanism of action is related to organic compounds containing heteroatoms (atoms other than hydrogen in their molecular structure) like oxygen (O), nitrogen (N), and sulfur (S) in their molecular structure. The existence of these atoms plays an important role in the increased affinity of the molecules to the surface of the metal, which in turn improves the adsorption and helps in building a better barrier to prevent corrosive reactions.

The success of corrosion inhibitors is largely based on the adsorption capability of the metal interface, and the adsorption mechanism governs the development of a protective layer over the corrosive species. The behaviour of this adhesion greatly relies on the electronic structure of the molecule used as an inhibitor, which can decide reactivity, distribution of charges and the potential of attachment to the metal surface. Furthermore, the interaction of the inhibitor with the metal is determined by the adsorption mechanism (physical or chemical); this basic difference eventually has a decisive influence on the overall efficiency of corrosion inhibition. Understanding these mechanisms is crucial for the creation of superior, eco-conscious and long-lasting corrosion-preventing agents (Wan-Nik *et al.*, 2010; Bertolini *et al.*, 2013; Zulkifli *et al.*, 2021). Nowadays, research efforts have been largely focused on enhancing the durability and environmental benefits of the inhibitors by exploring biodegradable, non-toxic alternatives that can reduce environmental impact while offering long-term protection for metal structures (Zhang *et al.*, 2016; Kamaruzzaman *et al.*, 2021; Kamaruzzaman *et al.*, 2022; Merimi *et al.*, 2023).

Specifically, material management strategies for extending the service life of structures have become increasingly important. Long-term durability and the prevention of corrosion are vital to the sustainable management of industrial assets. Our research team has previously explored various aspects of corrosion inhibition, identifying key factors that influence the inhibitory efficiency (EI%) of different chemical substances, placing specific emphasis on the function of organic inhibitors and their adsorption behaviour and electronic properties. These factors are essential for developing advanced, cost-effective, and sustainable solutions to combat corrosion.

To further advance this field and contribute toward the creation of enhanced and enduring corrosion-preventing agents, the current study systematically evaluates the corrosion inhibition performance of two organic compounds: Acetaminophen (A1) and acetylsalicylic acid (A2) (Zhang *et al.*, 2016; Abdallach *et al.*, 2002; Selma *et al.*, 2002). These inhibitors were tested on mild steel and carbon steel in a 1 M hydrochloric acid (HCl) solution, a common corrosive medium. The findings of this research aim to acquire critical comprehension into the efficiency, adsorption characteristics and potential mechanisms of action of these inhibitors, while also highlighting their potential as sustainable corrosion protectants. This research contributes to ongoing efforts to enhance corrosion protection, improve the durability of industrial materials, and promote environmentally friendly and long-term material management strategies in industrial applications.

Material and Method

Inhibitors Structure

The chemical structure of inhibitors acetaminophen (A1) and acetylsalicylic acid (A2) is illustrated in Figure 1.

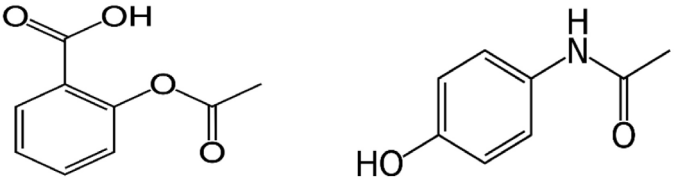

A1 A2

Figure 1: Chemical molecular structures of (A1) acetaminophen and (A2) acetylsalicylic acid

Materials

The initial metal examined was XC48 carbon steel, with a weight-based elemental composition of C = 0.48%, Mn = 0.66%, Si = 0.27%, Ni = 0.02%, Cr = 0.21%, Mo = 0.02%, and Fe = 98.21%. The other metallic material, identified as mild steel was characterised by the following elemental make-up by weight: C = 0.076%, Mn = 0.192%, Cr = 0.050%, Si = 0.026%, P = 0.012%, Cu = 0.135%, Al = 0.023%, and Ni = 0.05%, with the remainder being Fe. Both steel specimens were machined and prepared in the form of uniform parallelepiped samples with the dimension of 2.0 cm x 2.0 cm x 0.5 cm, in order to guarantee uniform surface area, controlled geometry, as well as reliable reproducibility during experiments. For each sample, the total exposed surface area was approximately 0.28 cm². The specimens were mounted in an inert resin for subsequent testing. Prior to each corrosion assay, the specimens were meticulously polished using sandpaper with abrasive grades extending from 100 to 2,000, followed by washing using purified water, and any residual corrosion inhibitors (A1 and A2) were removed using acetone. Lastly, each specimen was dried at 298 K to ensure a clean, dry surface before the corrosion testing (Verma *et al.*, 2021; Merimi *et al.*, 2023).

Solutions

The acidic medium consisting of 1.0 M HCl was prepared by diluting 37% reagent-grade HCl using distilled water. The inhibitors A1 and A2 were applied at concentrations ranging from 10^{-3} M.

Electrochemical Measurements

Electrochemical evaluation was performed systematically in aerated solutions at 308 K with the use of a Volta Lab potentiostat (Radiometer PGZ 100), under static condition control and continuous control of Voltester 4 software for the occurrence of reliable and repeatable data acquisition during the entire experimental programme. In this study, an experimental setup was used, comprising a common three-electrode corrosion system that consisted of a working electrode made of mild and XC48 steel with an exposed area of 0.32 cm², and a counter electrode made of platinum with an area of 1 cm² to complete the electrical circuit, with a Saturated Calomel Electrode (SCE) to act as a reliable reference. Before the actual electrochemical tests, the working electrode was introduced into the test solution and left to rest for 30 minutes to ensure that the open circuit potential (E_{ocp}) was fully stabilised and a steady-state condition was achieved. Then, after the E_{ocp} had settled to a steady state, all the electrochemical tests were done under the same conditions, making sure that measurements taken were consistent and could be compared.

The measurements of Electrochemical Impedance Spectroscopy (EIS) were performed within a frequency range between 100 kHz and 0.1 Hz at the open circuit potential with a continuous rms perturbation amplitude of 10 mV, which was driven into the system to probe the interfacial response without inducing significant changes to the system. The semicircular response that appears in the Nyquist plot was optimally fitted by applying non-linear least-squares adjustment on the experimental data

points to find the intersection with the x-axis with better precision. The effectiveness of corrosion prevention was then determined using the values of the charge transfer resistance (R_{ct}) as measured under each combination, as per Equation (1):

$$\eta\% = \frac{R^i - R^o}{R^i} \times 100 \quad (1)$$

where R° and R^i represent the R_{ct} without and with inhibitors, respectively. The analysis of potentiodynamic polarisation was conducted in the inhibited and uninhibited medium on the mild steel substrate, with the applied potential to the substrate moved gradually from the cathodic domain to the anodic domain over a range of 250 mV at a constant scan rate of 1 mV/s^{-1} to produce similar polarisation profiles. To determine the corrosion current densities (I_{corr}), the linear Tafel areas in the anodic and cathodic branches were extrapolated until they met each other at the corrosion potential. Then, the I_{corr} values were calculated by regressing the polarisation data on Equation (2):

$$I = Icorr[exp\ exp\ \left(\frac{2.3\Delta E}{ßa}\right) - exp\ exp\ \left(\frac{2.3\Delta E}{ßc}\right)] \quad (2)$$

The performance of the inhibitor was assessed by calculating the I_{corr} values according to Equation (3):

$$\eta Tafel\% = \frac{Icorr - Icorr(i)}{Icorr} \times 100 \quad (3)$$

DFT Computations

To further enhance the understanding of how molecular configurations and electronic characteristics affect corrosion inhibition mechanisms, a computational study of molecular properties using the DFT approach was employed. This computational methodology is essential for bridging experimental corrosion inhibition data with the chemical reactivity properties predicted through DFT. In the context of sustainability and long-term material management, these theoretical models can help identify environmentally friendly and efficient corrosion inhibitors that could extend the lifespan of materials while minimising their ecological impact. Molecular structures of the studied inhibitors were optimised in the gas and aqueous phases with the help of the Gaussian 09W software and DFT calculations were performed with the B3LYP functional and the 6-311G++(d,p) basis set to ensure a consistent and reliable electronic representation across the board (Zarrok *et al.*, 2012). Such computational methods offer significant understanding into the molecular-level interactions at the interface of inhibitors and metallic surfaces, which are critical for designing more durable and sustainable corrosion protection strategies.

Based on the optimised molecular configurations, an array of significant parameters was systematically derived, namely, electron density distributions with respect to the Highest Occupied Molecular Orbital (HOMO) or the Lowest Unoccupied Molecular Orbital (LUMO), and the obtained parameters were then utilised to calculate various other key physicochemical properties, such as the dipole moment, electronegativity, global softness and global hardness. By analysing these parameters, researchers can better understand the efficiency of inhibitors and tailor them for optimal performance, ensuring enhanced corrosion resistance over time and reduced environmental harm. The integration of DFT with experimental data plays a crucial role in developing corrosion inhibitors that not only enhance material durability but also align with sustainability goals. This approach allows for the design of inhibitors that offer long-term protection, reduce the frequency of maintenance and contribute to a more environmentally responsible management of industrial materials. Such research underscores the importance of adopting advanced computational tools to foster innovations in corrosion protection and material sustainability.

$$I = E(optimisedcation) - E(optimisedneutral) = - EHOMO \quad (4)$$

$$A = E(optimisedneutral) - E(optimisedanion) = - ELUMO \quad (5)$$

$$\chi = -\frac{1}{2}(EHOMO + ELUMO) \quad (6)$$

$$\eta = -\frac{1}{2}(EHOMO - ELUMO) \quad (7)$$

$$\sigma = \frac{1}{\eta} = \frac{-2}{EHOMO - ELUMO} \quad (8)$$

$$\Delta E = ELUMO - EHOMO \quad (9)$$

$$\Delta N = (\phi_{Fe} - \chi i_{nh})/2(\eta_{Fe} + \eta i_{nh}) \quad (10)$$

Wherein, the features of Fe are $\phi Fe = 4.82$ eV and $\eta Fe = 0$.

Molecular Dynamics (MD) Simulation Approach

The behaviour of a smooth metallic surface in contact with the chosen Schiff phenol bases was studied by MD simulations and the computational experiment was carried out in the Adsorption Locator module in the Material Studio 8.0 package to model the adsorption behaviour (licensed by BIOVIA, Dassault Systèmes). Moreover, DNP+ basis sets and suitable functionals of each component of the system were used. All the system elements' structures were optimised before the simulation.

This MD approach allowed the determination of adsorption and binding energies from the modelling regarding the interactions occurring between the iron surface and the inhibitor molecules. Materials Studio 8.0's Adsorption Locator module was employed for this purpose in a controlled computational setting (Sharma *et al.*, 2019). The structure of each inhibitor was first optimised to its lowest energy structure prior to beginning the simulations. The computational model was made up of a Fe (110) crystalline surface and a 6.0 Å thick slab, a (10 × 10) supercell, and a 50 Å vacuum layer. In all simulations, the geometries of all the modelled systems were optimised in the gas phase condition and aqueous medium by parameters of the COMPASS II force field in a way to ensure that the structure refinement in all environments was uniform (Sun *et al.*, 1998).

Results and Discussion

Potentiodynamic Polarisation Curves

Figure 2 shows the potentiodynamic polarisation response of XC48 steel and mild steel in the 1.0 M HCl solution, under uninhibited conditions and under different concentrations of inhibitors (A1, A2, and A1 + A2 systems). Among the parameters of polarisation that have been extracted were corrosion potential (E_{corr}), corrosion current density (I_{corr}), and the anodic and cathodic Tafel slopes (βa and βc), which characterise the kinetics of the electrochemical reactions involved in each branch. Based on the plots of the Tafel fitted, the following parameters, along with the corresponding inhibition efficiency (EI%), were obtained and then summarised in Table 1.

The findings shown in Figure 2 prove that the addition of the inhibitors (A1, A2, and A1 + A2) significantly inhibits both the cathodic and anodic processes, suggesting a general decrease in the corrosion reaction kinetics for the tested medium. Presumably, the compounds hinder metal oxidation at the anode and impede hydrogen generation. Observations indicate that the E_{corr} of XC48 and mild steel showed a minor shift to a positive potential when the inhibitors were present, compared to XC48 and mild steel when immersed in the aggressive solution. Furthermore, both the I_{corr} of anodic and cathodic currents were diminished. These findings indicate that A1 and A2 were mixed-type inhibitors (Zhan *et al.*, 2016; Haque *et al.*, 2020; Merimi *et al.*, 2023).

When inhibitors were present, the I_{corr} values of the mild steel surface were lower, which indicated a clear reduction in the corrosion rate, while the combined formulation of A1 + A2 showed the highest EI%, as measured in Table 1. In addition, E_{corr} shifted toward more positive potentials when inhibitors were present in comparison to the uninhibited state, indicating a measurable change in corrosion potential. The combination of the inhibitors improved EI% in both types of steel. The EI% of A1 + A2 was 94% in the case of XC48 and 97% in the case of mild steel, at a concentration of 10^{-3} M.

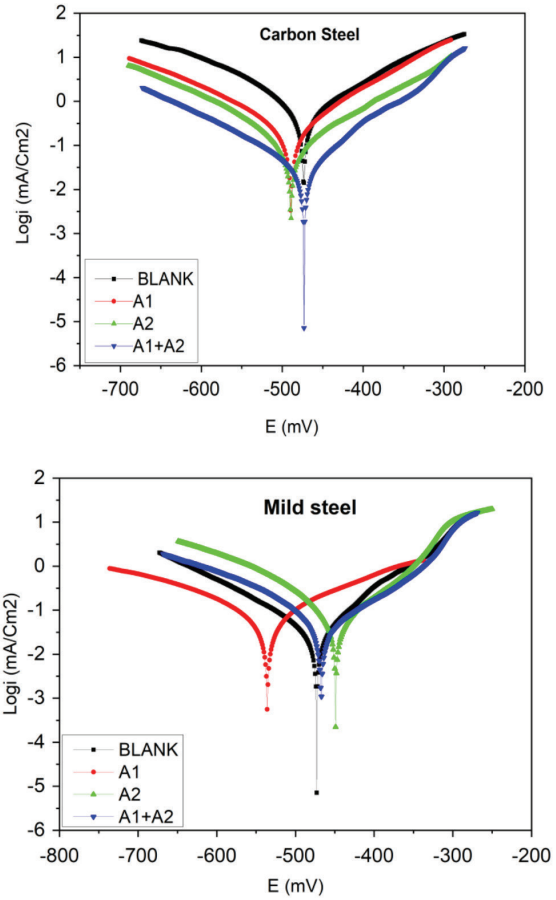

Figure 2: Polarisation profiles of carbon steel and mild steel in 1.0 M HCl, measured both without inhibitors and with 10^{-3} M concentrations of A1, A2, and A1 + A2

Table 1: The electrochemical parameters corresponding to mild steel in a 1.0 M HCl solution (at 308 K) without inhibitors and in the presence of different inhibitor concentrations

Inhibitors		**Conc (M)**	***-Ecorr* (mVSCE)**	**$-\beta_a$ (mV dec^{-1})**	**$-\beta_c$ (mV dec^{-1})**	**I_{corr} (mA cm^{-2})**	**ηTafel (%)**
HCl 1M	XC48	1.0	470	107.6	95.6	0.6216	-
	Mild steel	1.0	452	172.7	180.7	3.0063	-
A1	XC48	5.10^{-3}	484.6	89	99.6	0.18	71.04
	Mild steel	5.10^{-3}	448	98.6	189.1	0.32	89.35
A2	XC48	5.10^{-3}	463.8	66.5	94	0.0365	93.46
	Mild steel	5.10^{-3}	447.2	83.9	176	0.2313	92.3
A1 + A2	XC48	5.10^{-3}	469.9	81.2	106.5	0.0329	94.70
	Mild steel	5.10^{-3}	467.2	84.4	130	0.0785	97.67

EIS studies

The Nyquist plane measurements of impedance were done in order to assist in the interpretation of some of the inherent reaction mechanisms such as adsorption, diffusion, and charge transfer. Based on the Nyquist plots, the R_{ct}, C_{dl}, and the suppression effect were obtained with respect to the differences between the impedance at low and high frequencies corresponding to the real axis, in the manner that Tsuru and Jacquemin suggested (Tsuru *et al.*, 1978; Jacquemin *et al.*, 2010). When organic inhibitors were introduced to the acidic medium, the diameter of the depressed semicircle correspondingly increased and its size increased depending on the concentration of the inhibitors. The representative plots of Bode were plotted for carbon steel under different concentrations of A1, A2, and A1 + A2. The shape and magnitude of the impedance curves also changed in the high-impedance region, forming a concave semicircle. The frequency response analysis revealed that at intermediate concentrations of the inhibitors, the semicircle reflected a proportional inhibitory effect that was dependent on the type of steel, as illustrated in Figure 3.

As illustrated in Table 2, the results of the EIS analysis showed electrochemical parameters that revealed a definite rise in R_{ct} with a corresponding decline in C_{dl}. The given behaviour can be explained by the fact that the local dielectric constant becomes lower and/

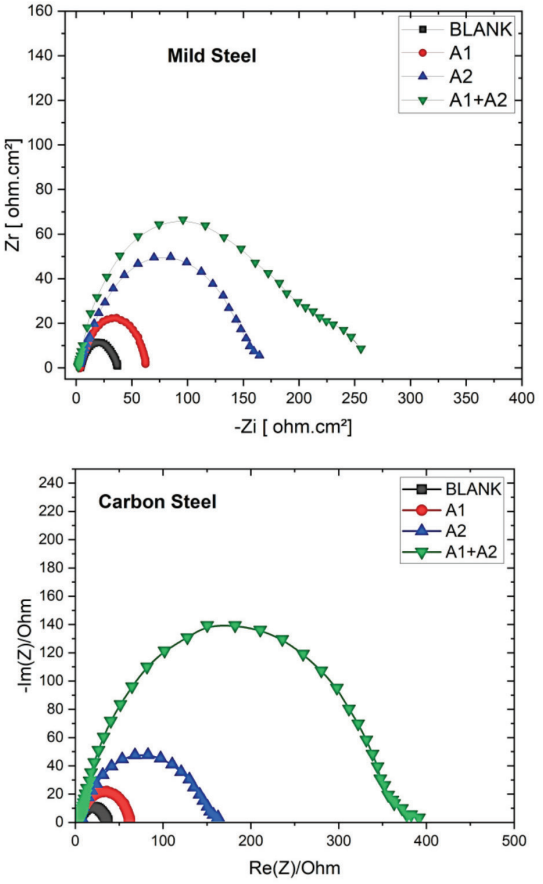

Figure 3: Impedance diagram of carbon and mild steel in 1 M HCl medium containing various compounds at 10^{-3}M

or there is an increase in the thickness of the electrical double layer at the interface. In general, these differences indicate that the molecules of the inhibitors act predominantly at the metal/solution interface, creating a protective film, which suppresses the charge transfer processes.

Scanning Electron Microscopy (SEM)

The morphology of the carbon steel and mild steel samples was extensively analysed with the help of SEM, which offers additional and more comprehensive information about the inhibition mechanism since the changes in the presence of the inhibitor on the exposed surfaces of the metals can be observed clearly (Özkır *et al.*, 2012; Oguzie *et al.*, 2014). The micrographs of the XC48 carbon steel and mild steel surfaces, after the samples had been exposed for six hours at 25°C in a 1 M HCl solution are shown in Figure 4. These images were taken both with and without inhibitors present (A1 + A2) at a concentration of 10^{-3}.

Theoretical Calculations (DFT)

Quantum modelling assessments were used to measure important molecular and electronic properties that affect EI%, and the likely charge interactions of the inhibitor molecules with the steel surface were predicted through a detailed analysis of the frontier molecular orbitals (Lgaz

Table 2: EIS parameters for the corrosion of carbon and mild steel in 1.0 M HCl at 308 K

Inhibitors	Conc (M)	R_{ct} (Ω cm^2)	f_{max} (Hz)	C_{dl} (µF cm^{-2})	EI (%)
HCl 1 M	1.0	15.27	108.7	95.82	-
Carbon steel A1 + A2	1.10^{-6}	51.26	49.8	62.1	68.26
	1.10^{-5}	70.42	50	45.2	76.89
	1.10^{-4}	89.43	50.2	35.59	81.81
	1.10^{-3}	155.12	31.64	32.43	89.51
Mild steel A1 + A2	1.10^{-6}	65.1	40	61.12	75.01
	1.10^{-5}	73.12	40	54.41	77.75
	1.10^{-4}	98.65	40	40.33	83.51
	1.10^{-3}	104.96	40	37.91	84.5

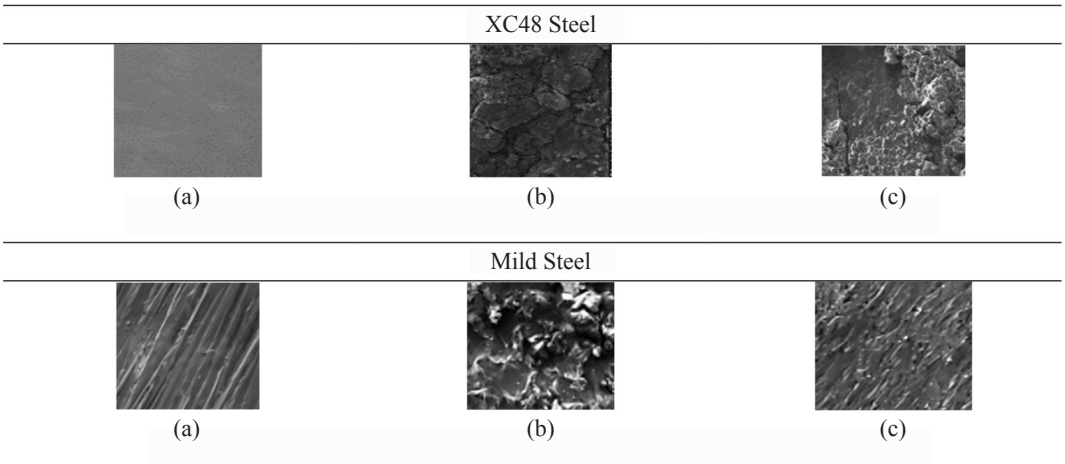

Figure 4: Micrographs (SEM) of the surface of carbon and mild steel after six hours of immersion in (b) 1 M HCl and (c) 1 M HCl + A1 + A2 at 10^{-3} M

et al., 2019). Optimised molecular structures of A1 and A2 and their Molecular Electrostatic Potential Surfaces (MEPS) and density distributions of HOMO and LUMO orbitals are shown in Figure 5.

The evaluated quantum chemical descriptors are summarised in Table 3. The ability of a molecule to donate or accept electrons was determined based on Frontier Orbital Theory, which is dependent on the energies of the HOMO and LUMO orbitals. It is widely recognised that the energy gap (E_{gap}) is associated with molecular stability, and consequently, with its reactivity (Kumar *et al.*, 2017). The lesser the value of E_{gap} is the greater the reactivity of the molecule, and this is one of the characteristics that a very good corrosion inhibitor must have. The effectiveness of the inhibitors could be evaluated as a consequence of the spatial distribution of the frontier molecular orbitals displayed graphically as those of HOMO and LUMO. Despite the resemblance in the structure of Schiff bases, their functional groups include single or combinations of -OCH_3, -CHO, -NH and -OH, which bring about differences. The LUMO and HOMO electron density of the two molecules was spread across all the functional groups, as indicated in Figure 5.

	A1	A2
Structures	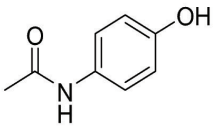 Acetaminophen (A1)	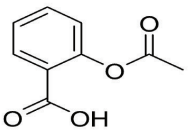 Acetylsalicylic(A2)
Optimised structures	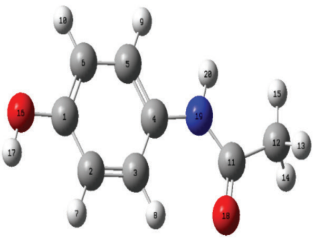	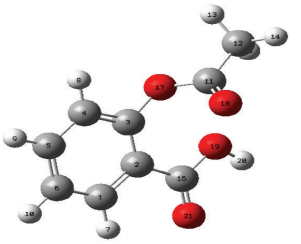
HOMO	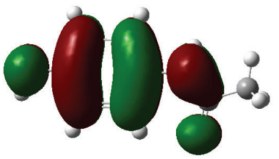	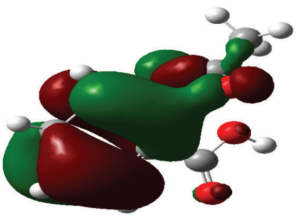
LUMO	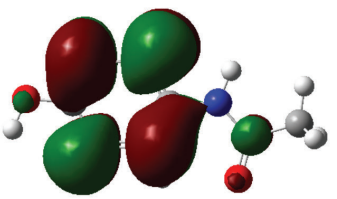	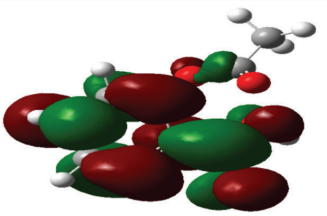

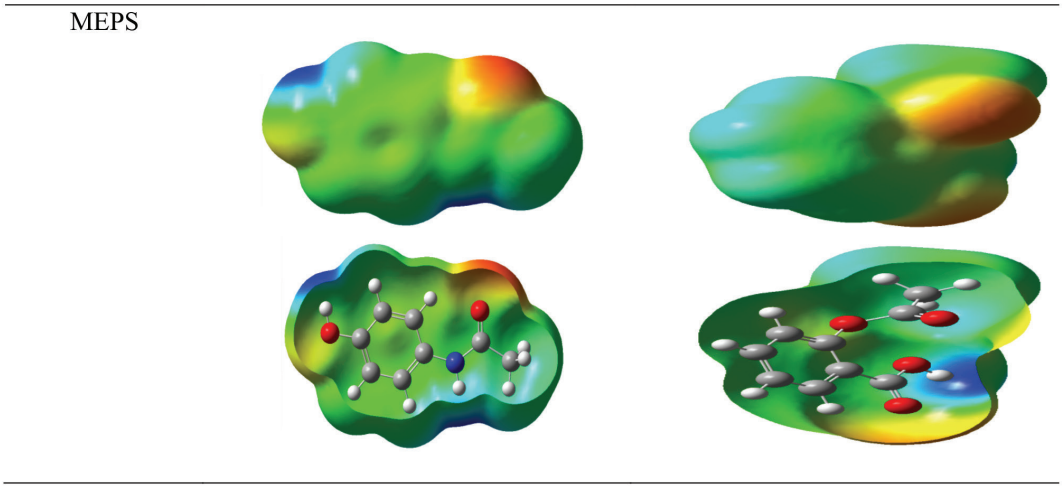

Figure 5: The optimised structures, LUMO, HOMO, and MEPS of PSB3 and PSB4 in the aqueous phase, as calculated with DFT/B3LYP/6-311G(d,p)

Table 3: Quantum chemical data in aqueous phase for A1 and A2

Quantum Chemical Parameters	A1	A2
EHOMO (eV)	-5.8689	-7.3446
ELUMO (eV)	-0.6250	-1.9072
E_{gap} (eV)	5.2439	5.4374
IE (eV)	5.8689	7.3446
A (eV)	0.6250	1.9072
χ (eV)	3.2469	4.6259
η (eV)	2.6219	2.7187
μ (Debye)	2.3082	2.8848
Ω (eV)	1,0160	1,5305
σ (eV)	0.3814	0.3678
ΔN	0.7157	0.4366
ΔE_{b-d}	0.6554	0.6796

Given that these groups are also understood to have critical functions in inhibitory activity, all compounds are anticipated to have strong electron-donating and electron-accepting activity. Accordingly, influences of individual functional groups on HOMO–LUMO distributions on minor differences were observed. In particular, electron-donating groups (hydroxyl) were found to exert a notable influence on the reactivity of the inhibitor molecules. Nonetheless, this specific occurrence has yet to be comprehensively explained by the frontier orbital distributions alone. Quantum chemical parameters were analysed to provide a clearer prediction of molecular reactivity and the role of functional groups. The greater the HOMO energies, the more electronic donating power was shown, and the lower the LUMO energies, the greater the electronic accepting power. The results in Table 3 indicate that electron donation occurred in the order of A1 > A2, but electron acceptance occurred in the order A2 > A1. The

energy gap is one important quantum chemical parameter, and generally, the smaller the value of the gap, the greater the reactivity and the more the inhibitor would adsorb to the surface. As such, since the E_{LUMO} and E_{gap} values were in close agreement with experimental values of A2, this validates its better inhibitory performance.

Donation of the electrons towards the metal surface by the inhibitors was evidenced by the observation of positive ΔN values. Upon closer examination of these values, it was found that A1 possessed a higher electron-donating capacity compared to A2, a result that is in agreement with the earlier studies reported. The general process of corrosion prevention was found to involve two processes occurring simultaneously. Initially, electrons were transferred from the HOMO of the inhibitor molecules to the vacant 3d orbitals of the iron atoms, followed by a second step in which electrons from the filled 3d orbitals of iron were back-donated into the LUMO of the inhibitor molecules, thereby completing a bidirectional electron exchange process. The results reported in Table 3 further indicate that A2 showed a pronounced tendency for adsorption on the mild steel surface, as evidenced by the obtained back-donation energy values ($\Delta E_{b\text{-}d}$).

In addition, the ΔN parameter, representing the number of electrons donated from the inhibitor to the metal surface, was found to be positive for both A1 and A2, which supports the conclusion that these compounds predominantly act as electron donors during the inhibition process. However, the order predicted by ΔN favours A2, which contradicts the experimental results. This discrepancy may arise from other factors such as the inhibitors' molecular structures, the way they are in contact with the metal surface, or even the role of environmental variables, which require further investigation. In the context of sustainable material management, understanding these molecular-level interactions is crucial for designing corrosion inhibitors that not only improve the durability of materials but also minimise environmental impacts. By refining our knowledge of the corrosion inhibition mechanisms, we can better select and optimise inhibitors for long-term protection, minimising the need to change and maintain frequently while promoting the responsible use of resources in industrial applications.

MD Simulations

There are numerous reports on calculations performed using DFT, but these have not comprehensively explained the interaction mechanisms between inhibitors and a metal surface. In this sense, computational modelling of corrosion inhibition has been progressively relying on MD simulations, which have also been discovered to be an effective and potent tool to investigate the inhibitor behaviour on the molecular scale. These simulations allow for the analysis of interactions at the interface of inhibitors and a metal substrate when exposed to corrosive species, providing an accurate evaluation of adsorption processes (Singh *et al.*, 2018). Such developments permit researchers to improve the knowledge and prediction of how the metal surface interacts with the inhibitor molecules and to aid in the creation of new synthetic corrosion inhibitors. The MD simulation parameters applied to all compounds are also considered (Lgaz *et al.*, 2018; Obot *et al.*, 2019).

The additions of the corrosive species in such simulations are done primarily to better model the corrosion process. Figure 6 shows the side and top views of the most favourable adsorption arrangements of the two inhibitors onto the iron surface, and the relevant properties are tabulated in Table 4. Figure 6 shows that all the molecules of the inhibitors are flattened and are located at right angles to the Fe (110) surface. This alternative position of the inhibiting molecules on the metal surface facilitates a greater level of surface coverage, thus improving the general interaction of the inhibitors and the substrate. With such an arrangement, the free pair electrons and π-electrons at the active sites of the inhibitors can easily react with the empty d-orbitals of the iron atoms, forming a dense and thick protective layer.

The previous quantum chemical descriptors have hinted that A2 could exhibit a good corrosion inhibition ability, and this theoretical idea was also backed by the completely parallel alignment in the MD simulations. In addition to this, the MD simulation data provided a more detailed understanding of adsorption behaviour and spatial orientation of the inhibitor molecules on the metal surface, and the correct assessment of inhibitor performance should also consider the strength of adsorption, which is highly dependent on the intermolecular interactions between the inhibitor molecules and the Fe (110) surface plane.

The total energy of the inhibitor or adsorbate system is part of the parameters provided in Table 3, and it matches the sum of the energies of the species in the adsorbed state. On iron substrates exposed to acidic conditions, the inhibitors exhibited total energies in the sequence A2 < A1. These results offer an important understanding of how corrosion inhibitors adsorb onto metal surfaces, supporting the development of more efficient materials management strategies that enhance the durability of metal structures over the long term. Additionally, the environmental benefits of selecting corrosion inhibitors based on such simulations are significant, as they can lead to the use of less harmful chemicals that prolong the service life of materials, thereby minimising the frequency of replacements and maintenance, and thus decreasing resource consumption and waste generation.

The energy associated with the attachment of adsorbate species onto a substrate surface is defined as the adsorption energy (E_{ads}). It is a well-known fact that steel corrosion is prevented by adsorption. Based on this fact, adsorption energy may be used as a criterion to rank various inhibitor molecules (Singh *et al.*, 2018). All the adsorption energy values reported in Table 4 were found to be negative, indicating that the adsorption process occurs spontaneously (Rbaa *et al.*, 2020). From a theoretical perspective, the higher EI% of A2 can be attributed to its larger absolute adsorption energy value. Based on the calculated molecular properties listed in Table 4, both the reactivity and inhibition performance of the compounds follow the order A2 > A1. In this context, the A2-substrate system exhibited the greatest stability along with the strongest adsorption interaction. As a result, A2 was identified as a more effective corrosion inhibitor compared to A1, a conclusion that is fully supported by the experimental findings.

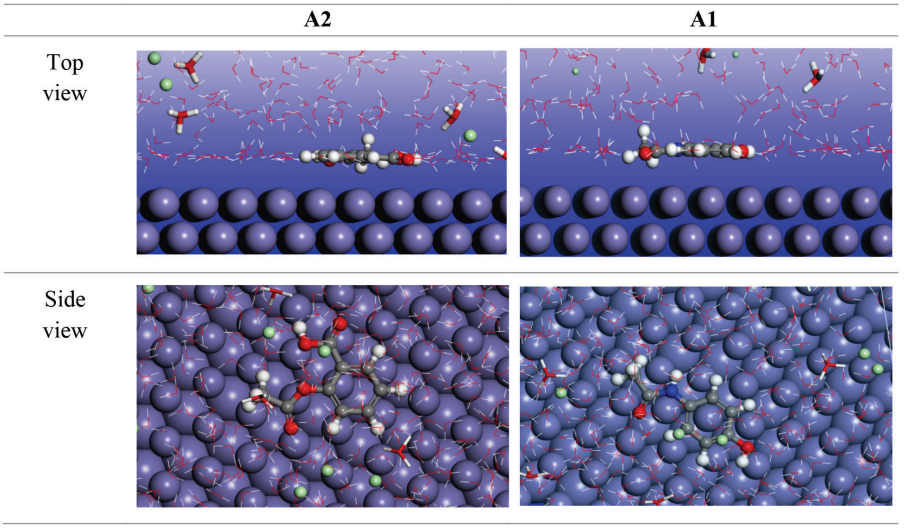

Figure 6: Graphical depictions of the most stable adsorption arrangements of both inhibitors on the Fe (110) surface, simulated in an environment containing 500 water molecules and 15 ($H_3O^+ + Cl^-$) ions

Table 4: MD simulation results for A1 and A2

Parameters (Kcal/mol)	System	
	Fe(110)/A1	Fe(110)/A2
Total energy	-150.005	-131.523
Adsorption energy	-89.050	-104.659
Rigid adsorption energy	-89.599	-102.208
Deformation energy	0.549	-2.450
Binding energy	-167.8	-178.6

Conclusions

The current study is a comprehensive evaluation of the corrosion preventive effectiveness of A1 and A2 as inhibitors for XC48 carbon steel and mild steel in 1.0 M HCl solution. To evaluate the effectiveness of these inhibitors, both experimental and theoretical methods were applied, including potentiodynamic polarisation, EIS, SEM, MD simulations, and DFT. The electrochemical measurements demonstrated that both A1 and A2 effectively inhibit corrosion by suppressing both anodic and cathodic reactions, leading to a movement of the corrosion potential toward more positive values and a decrease in I_{corr}. The EI% was highest when both inhibitors were used together, with an impressive EI% of 97% for mild steel and 94% for XC48 steel at a concentration of 10^{-3} M. According to these results, A1 and A2 are mixed-type inhibitors, effectively blocking the corrosion process degradation reactions through adsorption by adsorbing on the metal surface. The EIS data further confirmed the findings from the polarisation studies, indicating a rise in R_{ct} and a fall in C_{dl} when the inhibitors were introduced. These results show that the inhibitor molecules are adsorbed onto the metal surface, which strengthens the protective layer and curtails the further process of corrosion.

SEM analysis of the metal surfaces supported these findings, with the surface morphology indicating a protective layer formed by the inhibitors that prevented additional corrosion damage. Additional insight into the interactions between inhibitor molecules and the metal surface was provided through computational analyses, including DFT and MD simulations. The findings showed that the adsorption capacity of A2 and its association with the metal surface were superior to that of A1, which shows its high corrosion inhibition behaviour. To sum up, both experimental and theoretical findings emphasise the efficiency of both A1 and A2 in inhibiting corrosion on mild steel and XC48 carbon steel in acidic environments. These results help design more effective and environmentally friendly inhibitors to be used in industry, particularly in sectors where corrosion resistance is critical for the longevity of materials and infrastructure. The synergistic effect observed when both inhibitors are used together highlights the potential for optimising inhibitor formulations for enhanced corrosion protection, supporting long-term material durability and minimising environmental impacts.

Acknowledgements

We would like to acknowledge the Ministry of Higher Education Malaysia through Fundamental Research Grant Scheme (FRGS/1/2023/WAB05/UMT/02/1).

Conflict of Interest Statement

The authors declare no conflict of interest.

References

Abdallach, M. (2002). Rhodanineazosulpha drugs as corrosion inhibitors for corrosion of 304 stainless steel in hydrochloric acid

solution. *Corrosion Science*, *44*(4), 717–728. https://doi.org/10.1016/S0010-938X(01)00100-7

Al-Amiery, A. A., Betti, N., Isahak, W. N. R. W., Al-Azzawi, W. K., & Wan-Nik, W. M. N. (2023). Exploring the effectiveness of Isatin Schiff base as an environmentally-friendly corrosion inhibitor for mild steel in hydrochloric acid. *Lubricants*, *11*(5), 211. https://doi.org/10.3390/lubricants11050211

Bertolini, L., Elsener, B., Pedeferri, P., Redaelli, E., & Polder, R. B. (2013). *Corrosion of steel in concrete: Prevention, diagnosis, repair*. John Wiley & Sons. https://doi.org/10.1002/9783527651696

Dehri, I., & Özcan, M. (2006). The effect of temperature on the corrosion of mild steel in acidic media in the presence of some sulfur-containing organic compounds. *Materials Chemistry and Physics*, *98*(2–3), 316–323. https://doi.org/10.1016/j.matchemphys.2005.11.035

Eliboev, I., Berdimurodov, E., Yakhshinorov, L., Abdisattarov, J., Dagdag, O., Berisha, A., Wan-Nik, W. B., Kholikov, A., & Akbarov, K. (2023). Supramolecular corrosion protection: Ecofriendly synthesis and efficacy of a β-cyclodextrin/o-phenylenediamine complex. *Journal of the Taiwan Institute of Chemical Engineers*, *147*, 104944. https://doi.org/10.1016/j.jtice.2023.104944

Haque, J., Srivastava, V., Quraishi, M. A., Chauhan, D. S., Lgaz, H., & Chung, I. M. (2020). Polar group substituted imidazolium zwitterions as eco-friendly corrosion inhibitors for mild steel in acid solution. *Corrosion Science*, *172*, 108665. https://doi.org/10.1016/j.corsci.2020.108665

Jacquemin, D., Perpète, E. A., Ciofini, I., & Adamo, C. (2010). Assessment of functionals for TD-DFT calculations of singlet–triplet transitions. *Journal of Chemical Theory and Computation*, *6*(5), 1532–1537. https://doi.org/10.1021/ct1000166

Kamaruzzaman, W. M. I. W. M., Fekeri, M. F. M., Nasir, N. A. M., Hamidi, N. A. S. M., Baharom, M. Z., Adnan, A., Shaifudin, M. S., Abdullah, W. R. W., Nik, W. M. N. W., Suhailin, F. H., Matori, K. A., Kien, C. S., Zaid, M. H. M., & Ghazali, M. S. M. (2021). Anticorrosive and microbial inhibition performance of a coating loaded with *Andrographis paniculata* on stainless steel in seawater. *Molecules*, *26*(11), 3379. https://doi.org/10.3390/molecules26113379

Kamaruzzaman, W. M. I. W. M., Nasir, N. A. M., Hamidi, N. A. S. M., Yusof, N., Shaifudin, M. S., Suhaimi, A. M. A. A. M., Badruddin, M. A., Adnan, A., Nik, W. M. N. W., & Ghazali, M. S. M. (2022). 25 years of progress on plants as corrosion inhibitors through a bibliometric analysis using the Scopus database (1995–2020). *Arabian Journal of Chemistry*, *15*(4), 103655. https://doi.org/10.1016/j.arabjc.2021.103655

Kumar, R., Chahal, S., Kumar, S., Lata, S., Lgaz, H., Salghi, R., & Jodeh, S. (2017). Corrosion inhibition performance of chromone-3-acrylic acid derivatives for low alloy steel with theoretical modeling and experimental aspects. *Journal of Molecular Liquids*, *243*, 439–450. https://doi.org/10.1016/j.molliq.2017.08.048

Lgaz, H., Chung, I.-M., Salghi, R., Ali, I. H., Chaouiki, A., El Aoufir, Y., & Khan, M. I. (2019). On the understanding of the adsorption of fenugreek gum on mild steel in an acidic medium: Insights from experimental and computational studies. *Applied Surface Science*, *463*, 647–658. https://doi.org/10.1016/j.apsusc.2018.09.001

Merimi, C., Hammouti, B., Zaidi, K., & Elmsellem, H. (2023). Comparative study of inhibitory efficacy of drug (acetaminophen) in 1 M HCl medium applied to carbon and mild steels. *Materials Today: Proceedings*, *72*, 3890–3895. https://doi.org/10.1016/j.matpr.2022.10.214

Merimi, C., Hammouti, B., Zaidi, K., Hafez, B., Elmsellem, H., Touzani, R., & Kaya, S. (2023). Acetylsalicylic acid as an environmentally friendly corrosion inhibitor for carbon steel XC48 in chloride environment. *Journal of Molecular Structure*, *1278*, 134883. https://doi.org/10.1016/j.molstruc.2022.134883

Merimi, C., Hmada, A., Hejjaj, C., Almutairi, S. M., Lgaz, H., Messali, M., Merimi, I., Dkhireche, N., Touhami, M. E., Touzani, R., & Hammouti, B. (2024). Investigating the potency of new imidazolium ionic liquids in preventing carbon steel corrosion in acidic conditions: An integrated experimental and DFTB semi-empirical approach. *Inorganic Chemistry Communications*, *167*, 112802. https://doi.org/10.1016/j.inoche.2024.112802

Merimi, C., Zaidi, K., Hammouti, B., Guo, L., Kaya, S., Elmsellem, H., Bouklah, M., & Touzani, R. (2022). Alpha-linoleic acid (ALA) as a corrosion inhibitor for XC48 steel in H2SO4 medium: An experimental and computational study. *International Journal of Corrosion and Scale Inhibition*, *11*(4), 1456–1482. https://doi.org/10.17675/2305-6894-2022-11-4-3

Obot, I. B., Haruna, K., & Saleh, T. A. (2019). Atomistic simulation: A unique and powerful computational tool for corrosion inhibition research. *Arabian Journal for Science and Engineering*, *44*(1), 1–32. https://doi.org/10.1007/s13369-019-03715-4

Oguzie, E. E., Chidiebere, M. A., Oguzie, K. L., Adindu, C. B., & Momoh-Yahaya, H. (2014). Biomass extracts for materials protection: Corrosion inhibition of mild steel in acidic media by *Terminalia chebula* extracts. *Chemical Engineering Communications*, *201*(6), 790–803. https://doi.org/10.1080/00986445.2013.790816

Özkır, D., Kayakırılmaz, K., Bayol, E., Gürten, A. A., & Kandemirli, F. (2012). The inhibition effect of Azure A on mild steel in 1 M HCl. A complete study: Adsorption, temperature, duration, and quantum chemical aspects. *Corrosion Science*, *56*, 143–152. https://doi.org/10.1016/j.corsci.2011.11.010

Rbaa, M., Benhiba, F., Dohare, P., Lakhrissi, L., Touir, R., Lakhrissi, B., Zarrouk, A., & Lakhrissi, Y. (2020). Synthesis of new epoxy glucose derivatives as non-toxic corrosion inhibitors for carbon steel in molar HCl: Experimental DFT and MD simulation. *Chemical Data Collections*, *27*, 100394. https://doi.org/10.1016/j.cdc.2020.100394

Selma, L., Walid, D., Abdelmalik, E. A., Omar, D., Avni, B., Asma, B., Wan, W. B., Abdelkader, Z., & Abdellatif, L. (2023). Comparative study of the performance and inhibitory efficiency of two new organic heterocyclic in the chemical industry. *Materials Science and Engineering, B*, *297*, 116779. https://doi.org/10.1016/j.mseb.2023.116779

Sharma, S., Kumar, P., & Chandra, R. (2019). Applications of BIOVIA materials studio, LAMMPS, and GROMACS in various fields of science and engineering. In Sharma, S. (Ed.), *Molecular dynamics simulation of nanocomposites using BIOVIA materials studio, Lammps and Gromacs* (pp. 329–341). https://doi.org/10.1016/B978-0-12-816954-4.00007-3

Singh, A., Ansari, K. R., Quraishi, M. A., Lgaz, H., & Lin, Y. (2018). Synthesis and investigation of pyran derivatives as acidizing corrosion inhibitors for N80 steel in hydrochloric acid: Theoretical and experimental approaches. *Journal of Alloys and Compounds*, *762*, 347–362. https://doi.org/10.1016/j.jallcom.2018.05.236

Sun, H., Ren, P., & Fried, J. R. (1998). The COMPASS force field: Parameterization and validation for phosphazenes. *Computational and Theoretical Polymer Science*, *8*(1–2), 229–246. https://doi.org/10.1016/S1089-3156(98)00042-7

Tsuru, T., Haruyama, S., & Gijustsu, B. (1978). Corrosion inhibition of iron by amphoteric surfactants in 2M HCl. *Journal of Japan Society for Corrosion Engineering*, *27*, 573.

Verma, C., Ebenso, E. E., Quraishi, M. A., & Hussain, C. M. (2021). Recent developments in sustainable corrosion inhibitors: Design, performance and industrial scale applications. *Materials Advances*, *2*(12), 3806–3850. https://doi.org/10.1039/D0MA00681E

Wan-Nik, W. B., Sulaiman, O., Eng Giap, S. G., & Rosliza, R. (2010). Evaluation of inhibitive action of sodium benzoate on corrosion behaviour of AA6063 in seawater. *International Journal of Technology*, *1*(1), 20–28. https://doi.org/10.14716/ijtech.v1i1.39

Zarrok, H., Al Mamari, K., Zarrouk, A., Salghi, R., Hammouti, B., Al-Deyab, S. S., Essassi, E. M., Bentiss, F., & Oudda, H. (2012). Gravimetric and electrochemical evaluation of 1-allyl-1H-indole-2, 3-dione of carbon steel corrosion in hydrochloric acid. *International Journal of Electrochemical Science*, *7*(10), 10338–10357. https://doi.org/10.1016/S1452-3981(23)16281-X

Zhang, D., Tang, Y., Qi, S., Dong, D., Cang, H., & Lu, G. (2016). The inhibition performance of long-chain alkyl-substituted benzimidazole derivatives for corrosion of mild steel in HCl. *Corrosion Science*, *102*, 517–522. https://doi.org/10.1016/j.corsci.2015.10.002

Zhang, Z., Tian, N. C., Huang, X., Shang, W., & Wu, L. (2016). Synergistic inhibition of carbon steel corrosion in 0.5 M HCl solution by indigo carmine and some cationic organic compounds: Experimental and theoretical studies. *RSC Advances*, *6*(27), 22250–22268. https://doi.org/10.1039/c5ra25359d

Zulkifli, M. F. R., Shamsul Bahrin, S. N., Abdullah, S., Mohd Ghazali, M. S., & Wan Nik, W. M. N. (2021). *Citrus aurantifolia* leaf extract as a potential anti-corrosion additive in alkyd paint for mild steel. *Journal of Sustainability Science and Management*, *16*(3), 10–20. http://doi.org/10.46754/jssm.2021.04.002